Chapter 9
Accelerator-Driven System (ADS) Study in Kyoto University Research Reactor Institute (KURRI)

Cheol Ho Pyeon

Abstract Experimental studies on the uranium- and thorium-loaded accelerator-driven system (ADS) are being conducted for basic research of nuclear transmutation analyses with the combined use of the core at the Kyoto University Critical Assembly (KUCA) and the fixed-field alternating gradient (FFAG; 100 MeV protons) accelerator in the Kyoto University Research Reactor Institute. The ADS experiments with 100 MeV protons were carried out to investigate the neutronic characteristics of ADS, and the static and kinetic parameters were accurately analyzed through both the measurements and the Monte Carlo simulations of reactor physics parameters. An upcoming ADS at KUCA could be composed of highly enriched uranium fuel and Pb-Bi material, and the reaction rate ratio analyses (^{237}Np and ^{241}Am) of nuclear transmutation could be conducted in the ADS (hard spectrum core) at KUCA. The neutronic characteristics of Pb-Bi are expected to be examined through reactor physics experiments at KUCA with the use of solid Pb-Bi materials at the target and in the core.

Keywords 100 MeV protons • ADS • FFAG accelerator • KUCA • Spallation neutrons • Tungsten target

9.1 Introduction

The accelerator-driven system (ADS) has been considered as an innovative system for the nuclear transmutation of minor actinides and long-lived fission products with the use of spallation neutrons obtained from the injection of high-energy protons into a heavy metal target. At the Kyoto University Critical Assembly (KUCA), a series of ADS experiments [1–5] was carried out by coupling with the fixed-field alternating gradient (FFAG) accelerator [6–8], and the spallation

C.H. Pyeon (✉)

Nuclear Engineering Science Division, Research Reactor Institute, Kyoto University, Asashiro-nishi, Kumatori-cho, Sennan-gun, Osaka 590-0494, Japan
e-mail: pyeon@rri.kyoto-u.ac.jp

neutrons generated by 100 MeV protons from the FFAG accelerator were success-fully injected into uranium- [1, 2, 4] and thorium-loaded [5, 7] cores.

In the ADS facility at KUCA, reactor physics experiments are being carried out to study the neutronic characteristics through the measurements of reactor physics parameters, including reaction rates, neutron spectrum, neutron multiplication, subcriticality, and neutron decay constant. Among these, neutron multiplication was considered as an important index to recognize the number of fission neutrons in the core induced by the external neutron source.

The mockup experiments [5] of thorium-loaded ADS carried out by varying the neutron spectrum and the external neutron source were aimed at investigating the influence of different neutron profiles on thorium capture reactions and the prompt and delayed neutron behaviors in the subcritical system. The results provided important effects of the neutron spectrum and the external neutron source on both static and kinetic parameters: the effect of the neutron spectrum was investigated by varying the moderator material in the fuel region, and that of external neutron source by injecting separately 14 MeV neutrons and 100 MeV protons into the thorium-loaded core varying the moderator. Before the subcritical experiments, a thorium plate irradiation experiment was carried out in the KUCA core to analyze the thorium capture and fission reactions in the critical system as a reference of the subcritical system, although the feasibility of ^{232}Th capture and ^{233}U fission reactions could be examined in the subcritical state.

In this chapter, experimental results of the uranium- and thorium-loaded ADS are shown. Accuracy was evaluated through the comparison between the experiments and the calculations of the Monte Carlo analyses through the MCNPX [9] code with ENDF/B-VII.0 [10], JENDL/HE-2007 [11], and JENDL/D-99 [12] libraries. The ADS static and kinetic experiments at KUCA are presented in Sect. 9.2, the results and discussion of the experiments and calculations in Sect. 9.3, and the conclusion of the study in Sect. 9.4.

9.2 Experimental Settings

9.2.1 Uranium-Loaded ADS Experiments

KUCA comprises two solid polyethylene-moderated thermal cores designated A and B and one water-moderated thermal core designated C. The A-core is mainly used for experiments of ADS basic research. The three cores are operated at a low mW power in the normal operating state; the maximum power is 100 W. The constitution and the configuration of the cores can be altered easily, and the coupling with the conventional Cockcroft-Walton type accelerator and with the FFAG accelerator has allowed conducting experiments separately with the use of 14 MeV neutrons from deuteron–tritium fusion reactions and 100 MeV protons with the heavy metal target, respectively.
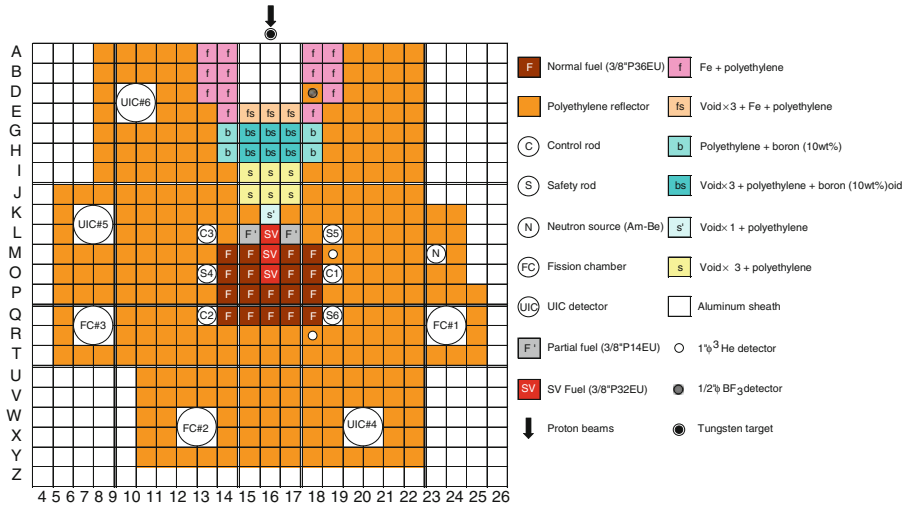
Fig. 9.1 *Top view* of the configuration of the A-core in the accelerator-driven system (ADS) experiments with 100 MeV protons
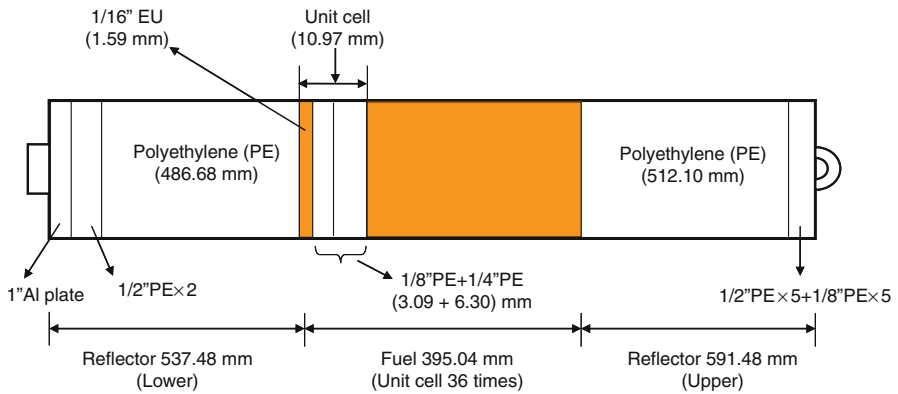

Fig. 9.2 *Side view* of of 3/8P″36EU fuel assembly (*F*, Fig. 9.1) in the A-core

The A-core (Fig. 9.1) employed in the ADS experiments was essentially a thermal neutron system composed of a highly enriched uranium fuel and the polyethylene moderator/reflector. In the fuel region, a unit cell is composed of the highly enriched uranium fuel plate 1/16 in. thick and polyethylene plates 1/4 in. and 1/8 in. thick (Fig. 9.2). The SV assembly is composed of a 5.08 × 5.08 × 5.08 cm center void region, 32 fuel unit cells, and the polyethylene blocks. In these ADS experiments, three types of fuel rods designated as the normal, partial, and special fuel SV were employed. For reasons of the safety regulations for KUCA, the heavy metal target was located not at the center of the core but outside the critical assembly. As in the previous ADS experiments with 14 MeV neutrons,
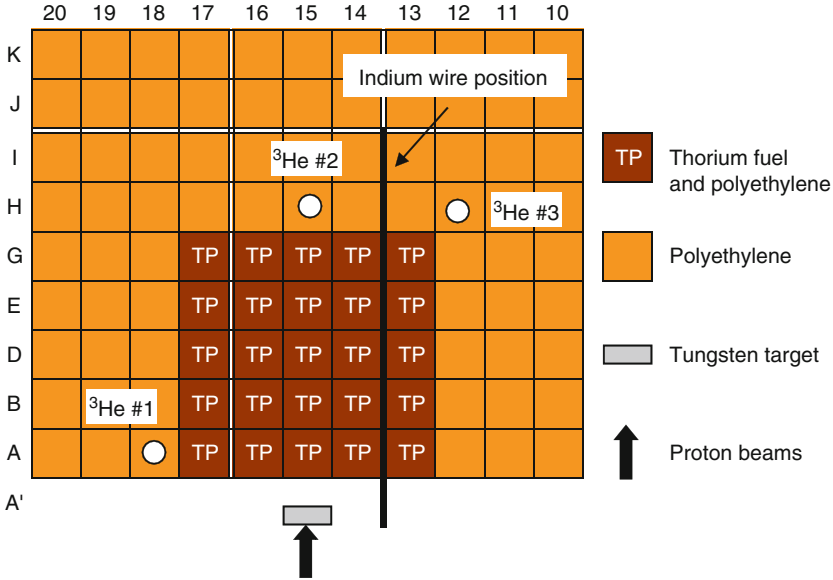
Fig. 9.3 *Top view* of thorium-loaded ADS core with 100 MeV protons

the introduction of a neutron guide and a beam duct is requisite to lead the high-
energy neutrons generated from the heavy metal target to the center of the core as
much as possible. In the uranium-loaded ADS experiments, the proton beam
parameters were 100 MeV energy, 0.01 nA intensity, 30 Hz pulsed frequency,
100 ns pulsed width, and 80-mm diameter spot size at the tungsten target (100 mm
diameter and 9 mm thick). The level of the neutron yield generated at the target was
around 1.0×10^6 1/s by the injection of 100 MeV protons onto the tungsten target.

9.2.2   Thorium-Loaded ADS Benchmarks

In the ADS with 100 MeV protons (Fig. 9.3), the fuel rod was composed of a
thorium metal plate and a polyethylene (PE), graphite (Gr), or beryllium
(Be) moderator arranged in the A-core. Other components were selected from
HEU and natural uranium (NU; $2 \times 2 \times 1/8$ in.) plates. The cores were composed
of Th-PE (Fig. 9.4), Th-Gr, Th-Be, Th-HEU-PE, and NU-PE, according to a
selection of moderator materials: PE, Gr, Be, HEU-PE, and NU-PE, respectively,
and spallation neutrons were generated outside the core after injection onto the
tungsten target. The thorium-loaded ADS experiments were conducted especially
to investigate the relative influence of different neutron profiles on capture reactions
of ^{232}Th and ^{238}U: the reaction of ^{238}U was taken as reference data for evaluating
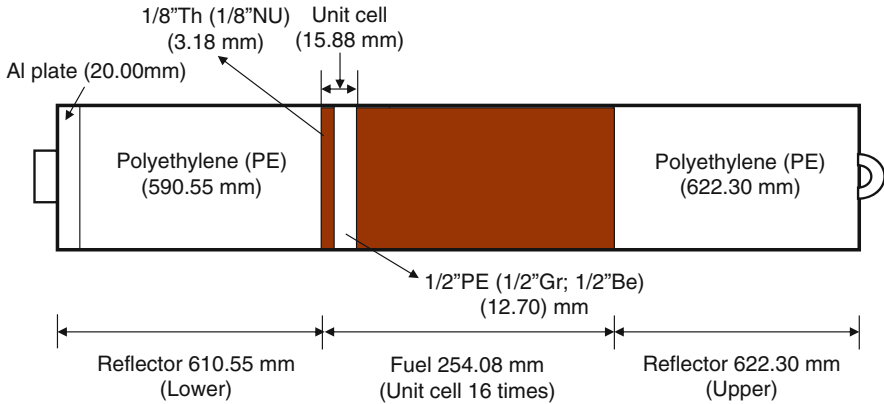the validity of ^{232}Th capture cross sections.

Fig. 9.4 *Side view* of Th-PE fuel assembly (TP) in thorium-loaded ADS core in Fig. 9.3

The main parameters of the proton beams were 100 MeV energy, 0.3 nA intensity, 20 Hz pulsed frequency, 100 ns pulsed width, and 40-mm-diameter spot size at the tungsten target (50 mm diameter and 9 mm thick). The level of the neutron yield generated at the target was around 1.0×10^7 1/s by the injection of 100 MeV protons onto the tungsten target.

Prompt and delayed neutron behavior was monitored by placing three ^{3}He detectors (20 mm diameter and 300 mm long) at three locations. Throughout the time evolution of the prompt and delayed neutrons, the prompt neutron decay constant was deduced by least-squares fitting to an exponential function over the optimal duration. Subcriticality was deduced by the extrapolated area ratio method [13] on the basis of prompt and delayed neutron behaviors. For 100 MeV protons, neutron detectors (^{3}He detectors: #1, #2, and #3) were set at three locations.

9.3 Results and Discussion

9.3.1 Uranium-Loaded ADS Experiments

9.3.1.1 Static Experiments

Thermal neutron flux distribution was estimated through the horizontal measurement of the ^{115}In$(n, \gamma)^{116m}$In reaction rate distribution by the foil activation method using an indium (In) wire 1.0 mm in diameter. The wire was set in an aluminum guide tube, from the tungsten target to the center of the fuel region [from the position of $(13, 14 - A)$ to that of $(13, 14 - P)$ (Fig. 9.1)], at the middle height of the fuel assembly. The experimental and numerical results of the reaction rates were normalized using an In foil $(20 \times 20 \times 2$ mm) emitted by ^{115}In$(n, n')^{115m}$In at the target. In this static experiment, the subcritical state $(0.77 \% \Delta k/k)$ was also attained
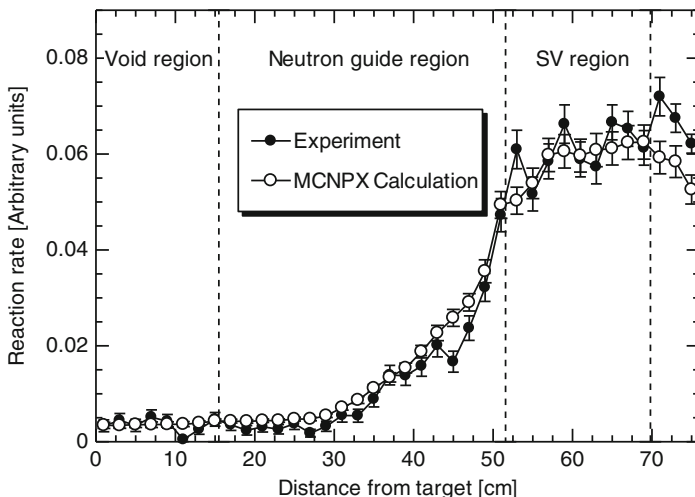
Fig. 9.5 Comparison of measured and calculated reaction rate distributions along the horizontal from (13, 14 – A) to (13, 14 – P) in Fig. 9.1 [2]

by the full insertion of C1, C2, and C3 rods. The numerical calculation was performed by MCNPX based on ENDF/B-VII.0. The generation of the spallation neutrons was included in the MCNPX calculation bombarding the tungsten target with 100 MeV proton beams. Because the reactivity effect of the In wire is considered to be not negligible, the In wire was taken into account in the simulated calculation: the reaction rates were deduced from tallies taken in the In wire setting region. The result of the fixed source calculation for the reaction rates was obtained after 2,000 active cycles of 100,000 histories, which led to a statistical error less than 10 % in the reaction rates. As shown in Fig. 9.5, the measured and the calculated reaction rate distributions were compared to validate the calculation method. The calculated reaction rate distribution agreed approximately with the experimental results within the statistical errors in the experiments, although these experimental errors were rather larger than those of the calculations. These larger errors in the experiments were attributed to the status of the proton beams described in Sect. 9.2.1, including the weak beam intensity and the poor beam shaping at the target.

9.3.1.2 Kinetic Experiments

To obtain information on the detector position dependence of the prompt neutron decay measurement, the neutron detectors were set at three positions as shown in Fig. 9.1: near the tungsten target [position of (17, D): 1/2-in.-diameter BF_3 detector]; and around the core [positions of (18, M) and (17, R): 1-in.-diameter ^{3}He detectors]. The prompt and delayed neutron behaviors (Fig. 9.6) were
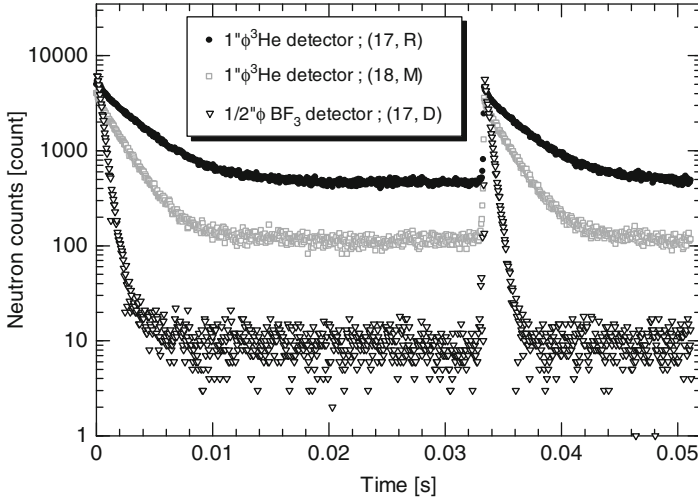
Fig. 9.6 Measured prompt and delayed neutron behaviors obtained from BF$_3$ and ^{3}He detectors in the A-core in Fig. 9.1 [2]

experimentally confirmed by observing the time evolution of neutron density in ADS, an exponential decay behavior and a slowly decreasing one, respectively. These behaviors clearly indicated that the neutron multiplication was caused by an external source: the sustainable nuclear chain reactions were induced in the sub-critical core by the spallation neutrons through the interaction of the tungsten target and the proton beams from the FFAG accelerator. In these kinetic experiments, the subcriticality was deduced from the prompt neutron decay constant by the extrapolated area ratio method. The difference of measured results of 0.74 %$\Delta k/k$ and 0.61 %$\Delta k/k$ at the positions of (17, R) and (18, M) in Fig. 9.1, respectively, from the experimental evaluation of 0.77 %$\Delta k/k$, which was deduced from the combination of both the control rod worth by the rod drop method and its calibration curve by the positive period method, was within about 20 %. Note that the subcritical state was attained by a full insertion of C1, C2, and C3 control rods into the core.

9.3.2 Thorium-Loaded ADS Experiments

9.3.2.1 Static Experiments

the profile of neutron flux for the ^{232}Th capture reactions was estimated through the horizontal measurement of ^{115}In(n, γ)^{116m}In reaction rate distribution, as well as described in Sect. 9.3.1.1. The wire was set in an aluminum guide tube, from the tungsten target to the center of the fuel region [from the position of (13, 14 – A′) to that of (13, 14 – I); Fig. 9.3], at the middle height of the fuel assembly. The absolute values of the measured reaction rates (Fig. 9.7) revealed differently the variation of
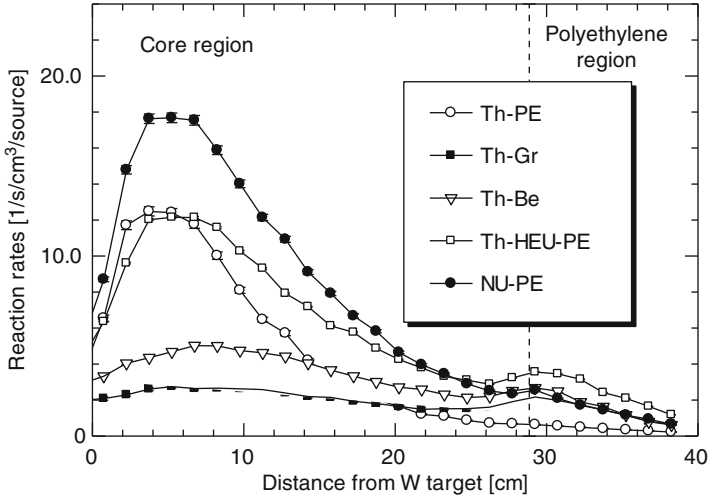
Fig. 9.7 Measured ^{115}In$(n, \gamma)^{116m}$In reaction rates obtained from the thorium-loaded ADS experiments with 100 MeV protons [5]

reaction rates attributed to varying the neutron spectrum in the core, when the spallation neutrons generated by 100 MeV protons were injected into the core. The moderating effect of the high-energy neutrons in some cores (Th-PE, Th-HEU-PE, and NU-PE: $k_{eff} = 0.00613$, 0.58754, and 0.50867, respectively) was observed around the boundary between the core and polyethylene regions. The ^{115}In$(n, \gamma)^{116m}$In reaction rates in the NU-PE core were higher than in other cores, demonstrating, that the reaction rates of ^{238}U in the NU-PE core were larger than those of ^{232}Th in the thorium cores with the use of 100 MeV protons. Additionally, the effect of the neutron spectrum on the reaction rates was observed with 100 MeV protons by comparing the measured results of reaction rates shown in Fig. 9.5. Thus, an expected physical effect was indeed observed as a result of the neutron spectrum change obtained by varying the moderator materials in the fuel assembly. Additionally, the accuracy [5] of experimental and numerical analyses was compared successfully with the ratio (C/E) of calculations and experiments around the relative difference of 10 %, through the subcritical parameter of neutron multiplication M.

9.3.2.2 Kinetic Experiments

The time evolution of prompt and delayed neutron behaviors was examined through the injection of an external neutron source (Fig. 9.8). In the Th-HEU-PE core, the prompt neutron decay constant (Table 9.1) at ^{3}He detector #1 was different from those at the others by the least-squares fitting, regardless of the kind of external neutron source and the position of neutron detection. It was considered overestimated, especially at detector #1, which was located near the external
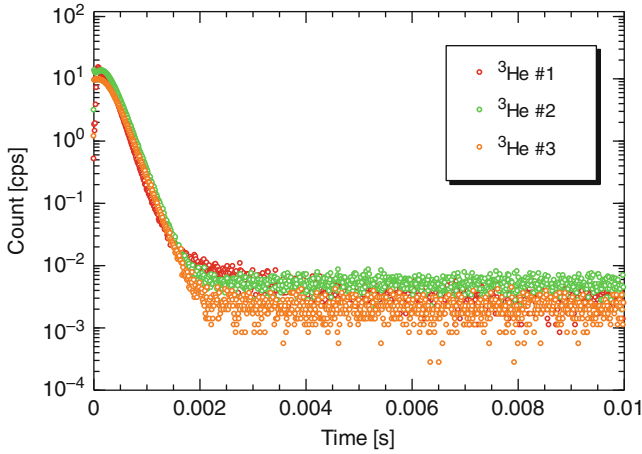
Fig. 9.8 Measured prompt and delayed neutron behaviors obtained from the thorium-loaded ADS experiments with 100 MeV protons (Th-HEU-PE)

Table 9.1 Measured results of prompt neutron decay constant (α [1/s]) in Th-HEU-PE core

Source	^{3}He #1	^{3}He #2	^{3}He #3
14 MeV neutrons	$5,735 \pm 5$	$5,155 \pm 4$	$5,161 \pm 4$
100 MeV protons	$5,788 \pm 5$	$5,338 \pm 5$	$5,229 \pm 5$

Table 9.2 Measured results of subcriticality (dollar units) in Th-HEU-PE core by the extrapolated area ratio method

Source	^{3}He #1	^{3}He #2	^{3}He #3
14 MeV neutrons	12.36 ± 0.51	29.70 ± 0.03	61.28 ± 0.09
100 MeV protons	31.19 ± 0.15	26.00 ± 0.10	43.14 ± 0.24

neutron source. The two different neutron sources provided different delayed neutron backgrounds. Subcriticality in dollar units was deduced by the extrapolated area ratio method with the use of prompt and delayed neutron components, and experimentally evaluated according to the kind of external neutron source and the location of neutron detection. As is well known, these results revealed subcriticality dependence on both the kind of external neutron source and the location of neutron detection, although the value of subcriticality was theoretically unchanged, regardless of the external neutron source and the location of the detector. Consequently, the experimental results (Table 9.2) showed that the subcriticality in pcm units for 14 MeV neutrons ($k_{\text{eff}} = 0.6577$) was different from that for 100 MeV protons ($k_{\text{eff}} = 0.7319$); remarkably, the discrepancy was also observed between the experiments and calculations ($k_{\text{eff}} = 0.5876$), although the calculated value was evaluated with the use of MCNPX eigenvalue calculations (total number of histories, 1×10^8).

9.4   Conclusions

At KUCA, the ADS experiments with 100 MeV protons were carried out with the combined use of the KUCA A-core and the FFAG accelerator. The neutronic characteristics of ADS were investigated through experimental and numerical analyses of reaction rate distribution and subcriticality.

The thorium-loaded ADS study was conducted as observed by prompt neutron behavior and reaction rates through kinetic and static experiments, respectively. Further, experiments of thorium-loaded ADS were successfully carried out in the subcritical states with the use of an external neutron source (14 MeV neutrons and 100 MeV protons, respectively).

In the future, upcoming ADS experiments with 100 MeV protons could be carried out at the highly enriched uranium-fueled and Pb-Bi-zoned core of KUCA to investigate the neutronic characteristics of Pb-Bi solid materials used in the core and at the target. Also, irradiation experiments of ^{237}Np and ^{241}Am could be conducted in the hard-spectrum core at KUCA to examine the feasibility of reaction rate ratio (capture/fission) conversion analyses of nuclear transmutation.

References

1. Lim JY, Pyeon CH, Yagi T et al (2012) Subcritical multiplication parameters of the accelerator-driven system with 100 MeV protons at the Kyoto University Critical Assembly. Sci Technol Nucl Install 395878:9
2. Pyeon CH, Misawa T, Lim JY et al (2009) First injection of spallation neutrons generated by high-energy protons into the Kyoto University Critical Assembly. J Nucl Sci Technol 46:1091–1093
3. Pyeon CH, Lim JY, Takemoto Y et al (2011) Preliminary study on the thorium-loaded accelerator-driven system with 100 MeV protons at the Kyoto University Critical Assembly. Ann Nucl Energy 38:2298–2302
4. Pyeon CH, Azuma T, Takemoto Y et al (2013) Experimental analyses of spallation neutrons generated by 100 MeV protons at the Kyoto University Critical Assembly. Nucl Eng Technol 45:81–88
5. Pyeon CH, Yagi T, Sukawa K et al (2014) Mockup experiments on the thorium-loaded accelerator-driven system at the Kyoto University Critical Assembly. Nucl Sci Eng 177:156 (in press)
6. Lagrange JB, Planche T, Yamakawa E et al (2013) Straight scaling FFAG beam line. Nucl Instrum Methods A 691:55–63

7. Planche T, Lagrange JB, Yamakawa E et al (2011) Harmonic number jump acceleration of muon beams in zero-chromatic FFAG rings. Nucl Instrum Methods A 632:7–17
8. Yamakawa E, Uesugi T, Lagrange JB et al (2013) Serpentine acceleration in zero-chromatic FFAG accelerators. Nucl Instrum Methods A 716:46–53
9. Pelowitz DB (2005) MCNPX User's manual, version 2.5.0. LA-CP-05-0369. Los Alamos National Laboratory
10. Chadwick MB, Obložinský P, Herman M et al (2006) ENDF/B-VII.0: next generation evaluated nuclear data library for nuclear science and technology. Nucl Data Sheets 107:2931–3060
11. Takada H, Kosako K, Fukahori T (2009) Validation of JENDL high-energy file through analyses of spallation experiments at incident proton energies from 0.5 to 2.83 GeV. J Nucl Sci Technol 46:589–598
12. Kobayashi K, Iguchi T, Iwasaki S et al (2002) JENDL dosimetry file 99 (JENDL/D-99). JAERI Report 1344
13. Gozani T (1962) A modified procedure for the evaluation of pulsed source experiments in subcritical reactors. Nukleonik 4:348